Published in final edited form as:
Eur Urol. 2010 June ; 57(6): 1030–1038. doi:10.1016/j.eururo.2009.10.020.

Morphologic Characterization of Preoperatively Treated Prostate Cancer: Toward a Post-Therapy Histologic Classification

Eleni Efstathiou, **Neil A. Abrahams**, **Rita F. Tibbs**, **Xuemei Wang**, **Curtis A. Pettaway**, **Louis L. Pisters**, **Paul F. Mathew**, **Kim-Anh Do**, **Christopher J. Logothetis**, and **Patricia Troncoso***
University of Texas, M. D. Anderson Cancer Center, Houston, Texas, USA

Abstract

Background—Preoperative treatment of prostate cancer (PCa) changes morphology of residual tumors so that the Gleason score is no longer valid.

Objective—To codify morphologic features of preoperatively treated PCa and identify potential classifiers predictive of outcome.

Design, setting, and participants—We performed a detailed morphologic evaluation of specimens obtained from 115 patients with high-risk PCa who had preoperative androgen ablation, alone or in combination with chemotherapy.

Measurements—Included hierarchical clustering analysis of morphologic characteristics, associations with other pathologic parameters, and univariate and multivariate analyses in search for associations with disease outcome.

Results and limitations—Based on hierarchical clustering analysis, we categorized pretreated prostate cancer in three morphologically distinct groups: group A, characterized by a predominance of cell clusters, cell cords, and isolated cells; group B tumors, by intact and fused small glands; and group C tumors by any degree of cribriform growth pattern or intraductal tumor spread.

Univariate analysis identified associations between this grouping, pathologic tumor stage ($p < 0.01$) and residual tumor volume ($p < 0.001$). Presence of intraductal spread or cribriform pattern in biopsies was associated with group C tumors. The presence of cribriform or intraductal spread morphology

*Corresponding author: Department of Pathology, The University of Texas M. D. Anderson Cancer Center, 1515 Holcombe Blvd., Unit 85, Houston, TX 77030 USA, Tel. +1 713 794 5449, Fax: +1 713 745 0778, ptroncos@mdanderson.org.

Author contributions: Patricia Troncoso had full access to all the data in the study and takes responsibility for the integrity of the data and the accuracy of the data analysis.
Study concept and design: Efstathiou, Logothetis, Troncoso.
Acquisition of data: Tibbs, Abrahams, Pisters, Pettaway, Troncoso.
Analysis and interpretation of data: Efstathiou, Wang, Troncoso.
Drafting of the manuscript: Efstathiou, Troncoso.
Critical revision of the manuscript for important intellectual content: Logothetis, Troncoso, Mathew.
Statistical analysis: Wang.
Obtaining funding: Logothetis, Mathew.
Administrative, technical, or material support: Efstathiou.
Supervision: Troncoso, Logothetis.
Other (specify): None.

Financial disclosures: I certify that all conflicts of interest, including specific financial interests and relationships and affiliations relevant to the subject matter or materials discussed in the manuscript (eg, employment/affiliation, grants or funding, consultancies, honoraria, stock ownership or options, expert testimony, royalties, or patents filed, received, or pending), are the following: None.

and positive surgical margins were stronger predictors of biochemical relapse than pathologic stage on multivariate analysis. The number of specimens evaluated in this study was limited, and a prospective validation is warranted along with molecular studies to validate the proposed morphologic classifier.

Conclusions—If validated, this classification will introduce uniformity in the selection of tissue samples for biomarker studies, facilitate the comparison of trials among different institutions, and may provide a new prognostic tool for preoperatively treated PCa.

1. Introduction

Preoperative treatment for locally advanced disease has offered a means of evaluating new therapeutic agents alone or in combination with hormonal ablation in the context of clinical trials [1–3]. The preoperative treatment strategy provides a unique opportunity both to evaluate in situ the effects of novel therapies [1] and to identify potential biologic/molecular markers by studying tumor samples obtained before and after therapy.

Unfortunately, detailed morphologic analyses of prostatectomy specimens have revealed that preoperative androgen ablation and chemotherapy affects the tumor architecture so as to render the Gleason score of post-therapy specimens nonrepresentative of the disease and therefore not useful for assessing prognosis [4–12].

This study aimed to identify consistent, easily recognized, reproducible morphologic patterns in prostatectomy specimens that may be helpful in assessing prognosis for patients with prostate cancer (PCa) after preoperative treatment. Hierarchical cluster analysis of morphologic features of such specimens revealed three potential groupings, and we further found that one of those three groupings was associated with biochemical failure.

2. Materials and methods

2.1. Patient selection and eligibility criteria

This retrospective study included men with locally advanced high-risk PCa preoperatively treated on one of three institutionally approved clinical trials at the University of Texas M. D. Anderson Cancer Center. Patients had (1) clinical T1c or T2 PCa and Gleason score ≥8; (2) clinical T2b or T2c PCa, Gleason score ≥7, and serum prostate-specific antigen (PSA) concentration ≥10 ng/ml; or (3) clinical T3 disease.

2.2. Preoperative therapy

All patients had preoperative androgen ablation (luteinizing hormone–releasing hormone analogue and antiandrogen), alone (30 patients) or in combination with ketoconazole, doxorubicin, vinblastine, and estramustine (57 patients) or docetaxel and imatinib (28 patients), lasting 12–18 wk. Radical prostatectomy was performed within 1 mo of therapy completion.

2.3. Radical prostatectomy specimen processing

Prostatectomy specimens and lymph nodes were processed and evaluated in their entirety as previously described [13,14].

Tumor volume was determined by a three-dimensional estimation method [13]. Pathologic stage and margin status were assigned using the modified American Joint Committee on Cancer staging system [15].

2.4. Histopathologic analyses of radical prostatectomy specimens

Specimens were reviewed by two genitourinary pathologists three times. The first review served to familiarize with the spectrum of histopathologic changes. During the second review, features were scored as present or absent and, where appropriate, using a three-point scoring system [16]. The third review served as reproducibility validation.

The histologic features evaluated included architectural patterns, stromal characteristics, and cytologic features. Architectural patterns included (1) single cells, (2) cell clusters/cords and solid sheets, (3) small isolated glands, (4) fused glands, (5) cribriform pattern, and (6) intraductal spread [17,18].

Stromal features were (1) stromal increase, (2) increased cellularity, (3) increased vascularity, (4) stromal mucin, and (5) tissue spaces devoid of epithelial lining (referred to as “absent lining”). Up to three tumor foci were evaluated separately. Cytologic features included (1) presence of prominent nucleoli, (2) pyknosis, (3) apoptosis, (4) cytoplasmic clearing, and (5) vacuolization.

2.5. Patient follow-up

Clinical follow-up information was obtained from patient charts. Rise in postoperative serum PSA ≥0.2 ng/ml was considered biochemical relapse. At the time of analysis, follow-up is too short to allow assessment of other end points. Median follow-up was 4.1 yr (range: 0.7–8.9 yr).

2.6. Statistical analyses

Patient characteristics were summarized by median, range for continuous and frequency (%) for categorical variables. Hierarchical clustering analysis for histologic changes was performed based on the Manhattan distance (ie, sum of absolute differences) between objects [19]. Biochemical relapse-free survival time was calculated from surgery date to biochemical relapse, patient death, or last follow-up, whichever occurred first. Unadjusted biochemical relapse-free survival probabilities were estimated by the Kaplan-Meier method [20].

Unadjusted two-group biochemical failure-free survival comparisons were made with log-rank testing [21]. The Cox proportional hazards regression model [22] assessed predictors of biochemical relapse-free survival, with goodness of fit assessed by using the Grambsch-Therneau test, Martingale residual plots [23]. The multivariate Cox model was obtained by backward elimination of variables with a p value cutoff of 0.05 and then allowing any variable previously deleted to enter the final model if its p value was <0.05. Statistical analyses were carried out using S-Plus software (v.XX; Insightful Corp, Seattle, WA, USA) [24].

3. Results

3.1. Patient, tumor, and treatment characteristics

The median patient age was 59 yr (range: 41–72 yr). Most patients were white. Other characteristics were well balanced among the three treatment groups (data not shown). Tables 1 and 2 list the patient and pathologic characteristics. A large majority of patients (71%) had a pretreatment Gleason score of ≥8, and only 36% were found to have organ-confined disease.

3.2. Histopathologic analyses and hierarchical cluster analysis

Histologic evaluation of radical prostatectomy specimens showed that architectural patterns in the residual PCa were predominantly fused glands and cell clusters (each present in 110 of the 115 specimens [95.7%]), followed by isolated small glands (in 102 specimens [88.7%]).

Cribriform pattern and intraductal spread were present in >50% of the cases but extensive in 11% (13 of 115) (Table 3 and Fig. 1).

Exploratory hierarchical cluster analysis identified three distinct clusters of architectural patterns: cell clusters, cords, and isolated cells clustered, as did isolated small glands with fused glands. Cribriform pattern co-migrated with intraductal spread.

Hierarchical clustering analysis of stromal features segregated the samples into two discrete groups (data not shown). No discrete groups on the basis of cytologic changes were found. Based on these observations, we initially assigned preoperatively treated tumors to three distinct morphologic groups. Group A is defined by the dominance of cell clusters, cell cords, and isolated cells, group B by the dominance of small and fused glands, and group C by the presence of a cribriform pattern, intraductal spread, or both (Fig. 2). According to this definition, 8.7% of the tumors (10 of 115) were assigned to group A, 19% to group B (22 of 115), and 72% to group C (83 of 115). There was no difference in the distribution of the three groups among the three different therapeutic regimens. Group assignment was based on the characteristics of the dominant tumor focus. There were no cases of multifocal disease in which the nondominant foci would be grouped as C when the dominant foci was A or B.

3.3. Associations between classification group and pathologic parameters

We first explored associations of the suggested grouping with pathologic stage and tumor volume. A statistically significant association was identified between groups and both pathologic tumor stage ($p < 0.001$) (Table 4) and volume of dominant tumor focus ($p < 0.001$) (Fig. 3). Volume of the dominant focus ranged from 0.03 to 13.82 cm^3 (mean: 2.83 cm^3; median: 2.00 cm^3). Median tumor volume of the dominant focus was significantly different between groups ($p < 0.001$) (Fig. 3).

Sixty-six percent of tumors in group C (55 of 83) had seminal vesicle invasion (ypT3b) (27 of 83) or lymph node metastases (ypTanyN1) (28 of 83) versus 25% (8 of 33) in groups A and B combined (27% [3 ypT3b, 3 ypTanyN1 of 22] in group B and 20% in group A [2 ypT3b of 10]). Higher biopsy Gleason score (>7) and group C morphology were not associated. Presence of cribriform pattern and/or intraductal spread in available (85 of 115) pretreatment biopsies and group C morphology in prostatectomy specimens were associated ($p < 0.001$) (Table 4).

3.4. Associations between classification group and biochemical failure

We explored potential correlations of candidate grouping with PSA recurrence. Forty-two patients (37%) had evidence of biochemical failure at a median of 6.6 yr (95% confidence interval, 4.1 yr not reached). Thirty-eight had tumors classified as group C. Twenty-two of 32 patients (68.8%) with lymph node metastases and 14 of 41 patients (34.2%) with ypT3N0 disease had biochemical failure versus 6 of 42 patients(14.3%) with ypT2 disease. Interestingly, five of six patients with ypT2 tumors who had biochemical relapse had group C tumors (Table 5). Finally, eight patients with confirmed local recurrence or bone metastases had group C tumors. Both suggested that groups and pathologic stage correlated strongly with risk of biochemical failure as indicated by Kaplan-Meier estimates (Fig. 4a–4c): Approximately half the patients with group C tumors experienced biochemical relapse, whereas only 13% with group A or B tumors did (Table 5). Presence of tumor at surgical margins was a predictor of outcome (Fig. 4d), as reported for patients undergoing prostatectomy alone [25]. Presence of cribriform pattern of growth and/or intraductal spread in available biopsies (85 of 115) was also associated with outcome (Fig. 4e). Preoperative therapeutic regimen, biopsy Gleason score, and PSA concentration at diagnosis were not found to predict outcome. Clinical disease stage was marginally important on univariate analysis ($p = 0.05$).

The multivariate Cox proportional hazards model (Table 6) identified presence of cribriform or intraductal spread (group C) and tumor at the surgical margin as predictors of relapse. Pathologic stage did not predict biochemical relapse in multivariate analysis as well as other variables considered (age, clinical disease stage, biopsy Gleason score, tumor volume, and serum PSA concentration at the time of diagnosis). Incomplete data on pretreatment biopsies precluded inclusion in this analysis.

4. Discussion

Despite several descriptive reports of morphologic alterations caused by preoperative androgen ablation [4–12,26], few studies have attempted to classify preoperatively treated tumors, with the previous one dating >25 yr [26].

The wide spectrum of morphologic heterogeneity of preoperatively treated, high-grade PCa in itself poses challenge to developing a morphology-based classification system. The hierarchical cluster analysis of tumor architectural features conducted in the present study identified three distinct groups based on architectural features. We sought preliminary evidence in support of the clinical relevance of the proposed grouping. We found clear associations with traditional indicators of disease outcome such as pathologic stage and tumor volume. More importantly, multivariate analysis identified the presence of cribriform pattern or intraductal spread as a stronger predictor of biochemical relapse than pathologic stage, tumor volume, PSA level at diagnosis, and biopsy Gleason score.

The long natural history of PCa, even for high-risk disease, allowed only biochemical relapse to be used as a reliable surrogate for disease outcome. Nevertheless, our findings signify that classification based on presence of cribriform pattern and/or intraductal spread may reflect the phenotype of the remaining disease more accurately than does pathologic tumor stage. Notably, the eight patients who had local relapse, bone metastases, or lymph node disease, including those who have, to date, died of disease, all had tumors that would be classified in group C.

Only large cohorts and longer follow-up intervals performed through multi-institutional collaborations will confirm whether presence of any of the two patterns will suffice as a practical single morphologic classifier serving the purpose of initial surrogate of outcome. Moreover, if this predictive surrogate is confirmed, the common uncertainty as to whether the morphology of a lesion is consistent with intraductal spread or cribriform features would not affect the outcome, as the presence of either falls into the same category..

All patients were treated with androgen ablation alone or in combination with chemotherapy. Thus it remains to be determined whether the morphologic spectrum in these treated cancers resulted more from the specific therapy than from a universal property of the cancers themselves. However, androgen ablation downregulates the causal pathway of PCa progression, which supports the hypothesis that the proposed classification is an adequate surrogate of treatment effect [27]. Additionally, reports of preoperative trials with docetaxel alone mentioned similar post-treatment features [28]. Application of this classification to other therapeutic regimens and studies addressing its reproducibility will establish the utility of this approach in standardizing the pathologic reporting of preoperatively treated specimens.

5. Conclusions

It is beyond the scope of this study to address whether aspects of tumor morphology after treatment reflect biologic characteristics that are responsible for tumor resistance. However, several groups have noted that the presence of intraductal spread or intraductal carcinoma in untreated and treated tumors is associated with an adverse prognosis [12,17,18,29,30].

Translational studies of the molecular profiles of pretreated PCa are required to address this question.

The lethal phenotype of PCa encountered among patients with high-risk disease is not likely amenable to standard therapeutic approaches. Given that maximum therapeutic index should be sought in the early stages of disease, it is unfortunate that in the case of high-risk PCa, identification of the multimodality therapeutic strategy that will confer maximal benefit to a select patient remains elusive. For the advent of personalized medicine, it is of paramount importance to define a signature of response or resistance to therapy that will guide therapeutic decisions. The process of identifying candidate composites of this signature requires not necessarily large but definitely well-designed trials with a focus on tissue-based studies.

To date, neoadjuvant trials seem to have failed toward that end. One possible reason has been the unrealistic end point of complete pathologic remission. PCa does not seem to recapitulate the behavior of other solid tumors and thus, unlike breast or bladder cancer, does not completely regress with initial treatment; however, this does not necessarily translate to treatment failure. Furthermore, the long natural history of the disease weighs against conducting trials that require such long follow-up. This has resulted in fewer PCa neoadjuvant studies as compared with other solid tumors. The classifier we propose may provide an alternative approach if proven an adequate surrogate or even predictor of outcome. Furthermore, the application of this practical histopathologic classification for preoperatively treated PCa will likely allow comparison of data between different trials and institutions and help standardize methods used in the conduct and analysis of preoperative trials. More importantly, it may contribute toward identifying the signature of response or resistance to treatment. Further correlative molecular studies in the microenvironment of tumors with the presence of cribriform pattern of growth or intraductal spread, both prior to and post-treatment, will elucidate candidate pathways of resistance to treatment. Unraveling such associations and identifying novel candidate therapeutic targets will guide future therapeutic approaches.

Acknowledgments

Funding/Support and role of the sponsor: The study was funded by the NIH Prostate SPORE at The University of Texas M. D. Anderson Cancer Center (NCI P50 CA90270) and Novartis Pharmaceuticals. They participated in the design and conduct of the study and the collection of data.

The authors acknowledge Ina Prokhorova, MD, HT, HTL (ASCP), for expert technical assistance with the pathologic specimens and Brooke Roche and Kim Vu for assistance in preparing the illustrations and the manuscript.

References

1. Efstathiou E, Troncoso P, Wen S, et al. Initial modulation of the tumor microenvironment accounts for thalidomide activity in prostate cancer. Clin Cancer Res 2007;13:1224–31. [PubMed: 17317833]
2. Oh WK. The evolving role of chemotherapy and other systematic therapies for managing localized prostate cancer. J Urol 2003;170:S28–34. [PubMed: 14610407]
3. Pettaway CA, Pisters LL, Troncoso P, et al. Neoadjuvant chemotherapy and hormonal therapy followed by radical prostatectomy: feasibility and preliminary results. J Clin Oncol 2000;18:1050–7. [PubMed: 10694556]
4. Bullock MJ, Srigley JR, Klotz LH, Goldenberg SL. Pathologic effects of neoadjuvant cyproterone acetate on nonneoplastic prostate, prostatic intraepithelial neoplasia, and adenocarcinoma: a detailed analysis of radical prostatectomy specimens from a randomized trial. Am J Surg Pathol 2002;26:1400–13. [PubMed: 12409716]
5. Civantos F, Marcial MA, Banks ER, et al. Pathology of androgen deprivation therapy in prostate carcinoma. A comparative study of 173 patients. Cancer 1995;75:1634–41. [PubMed: 8826921]

6. Grignon DJ, Bostwick DG, Civantos F, Garnick MB, Gaudin P, Srigley JR. Pathologic handling and reporting of prostate tissue specimens in patients receiving neoadjuvant hormonal therapy: report of the pathology committee. Mol Urol 1999;3:193–8. [PubMed: 10851323]
7. Hellström M, Häggman M, Brändstedt S, et al. Histopathological changes in androgen-deprived localized prostatic cancer. Eur Urol 1993;24:461–5. [PubMed: 8287886]
8. Reuter VE. Pathological changes in benign and malignant prostatic tissue following androgen deprivation therapy. Urology 1997;49:16–22. [PubMed: 9123731]
9. Vailancourt L, Tetu B, Fradet Y, et al. Effect of neoadjuvant endocrine therapy (combined androgen blockade) on normal prostate and prostatic carcinoma. A randomized study. Am J Surg Pathol 1996;20:86–93. [PubMed: 8540613]
10. Polito M, Muzzonigro G, Minardi D, Montironi R. Effects of neoadjuvant androgen deprivation therapy on prostatic cancer. Euro Urol 1996;30:26–31.
11. Tetu B, Srigley JR, Boivin JC, et al. Effect of combination endocrine therapy (LHRH agonist and flutamide) on normal prostate and prostatic adenocarcinoma. A histopathologic and immunohistochemical study. Am J Surg Pathol 1991;15:111–20. [PubMed: 1989458]
12. Selli C, Montironi R, Bono A, et al. Effects of complete androgen blockade for 12 and 24 weeks on the pathological stage and resection margin status of prostate cancer. J Clin Pathol 2002;55:508–13. [PubMed: 12101195]
13. Chen ME, Johnston D, Reyes AO, Soto CP, Babaian RJ, Troncoso P. A streamlined three-dimensional volume estimation method accurately classifies prostate tumors by volume. Am J Surg Pathol 2003;27:1291–301. [PubMed: 14508390]
14. Sanchez-Ortiz RF, Troncoso P, Babaian RJ, Lloreta J, Johnston DA, Pettaway CA. African-American men with nonpalpable prostate cancer exhibit greater tumor volume than matched white men. Cancer 2006;107:75–82. [PubMed: 16736511]
15. Greene, FL.; Fleming, ID.; Fritz, AG.; Balch, CM.; Haller, DG.; Morrow, M. American Joint Committee on Cancer. Cancer Staging Manual. 6. New York, NY: Springer Verlag; 2002.
16. Van de Voorde WM, Elgamal AA, Van Poppel HP, Verbeken EK, Baert LV, Lauweryns JM. Morphologic and immunohistochemical changes in prostate cancer after preoperative hormonal therapy. A comparative study of radical prostatectomies. Cancer 1994;74:3164–75. [PubMed: 7526970]
17. McNeal JE, Yemoto CEM. Spread of adenocarcinoma within prostatic ducts and acini. Morphologic and clinical correlations. Am J Surg Pathol 1996;20:802–14. [PubMed: 8669528]
18. Cohen RJ, Wheeler TM, Bonkhoff H, Rubin MA. A proposal on the identification, histologic reporting, and implications of intraductal prostatic carcinoma. Arch Pathol Lab Med 2007;131:1103–109. [PubMed: 17616999]
19. Bartels PH, Montironi R, Scarpelli M, Bartels HG, Alberts DS. Knowledge discovery processing and data mining in karyometry. Anal Quant Cytol Histol 2009;31:125–36. [PubMed: 19634783]
20. Kaplan EL, Meier P. Nonparametric estimation from incomplete observations. J Am Statist Assoc 1958;53:457–81.
21. Mantel N. Evaluation of survival data and two new rank order statistics arising in its consideration. Cancer Chemother Rep 1966;50:163–70. [PubMed: 5910392]
22. Cox DR. Regression models and life tables (with discussion). J R Statist Soc Series B 1972;24:187–220.
23. Therneau, TM.; Grambsch, PM. Modeling survival data: extending the Cox model. New York, NY: Springer; 2000.
24. Venables, WN.; Ripley, BD. Modern Applied Statistics with S Plus. 3. New York, NY: Springer; 1999.
25. Yossepowitch O, Bjartell A, Eastham JA, et al. Positive surgical margins in radical prostatectomy: outlining the problem and its long-term consequences. Eur Urol 2009;55:87–99. [PubMed: 18838211]
26. Dhom G, Degro S. Therapy of prostatic cancer and histopathologic follow-up. Prostate 1982;3:531–42. [PubMed: 7155986]

27. Matsushima H, Goto T, Hosaka Y, Kitamura T, Kawabe K. Correlation between proliferation, apoptosis, and angiogenesis in prostate carcinoma and their relation to androgen ablation. Cancer 1999;85:1822–7. [PubMed: 10223578]

28. Magi-Galluzzi C, Zhou M, Reuther AM, Dreicer R, Klein EA. Neoadjuvant docetaxel treatment for locally advanced prostate cancer. A clinicopathologic study. Cancer 2007;110:1248–54. [PubMed: 17674353]

29. Rubin MA, de La Taille A, Bagiella EM, Olsson CA, O'Toole KM. Cribriform carcinoma of the prostate and cribriform prostatic intraepithelial neoplasia: incidence and clinical implications. Am J Surg Pathol 1998;22:840–8. [PubMed: 9669346]

30. Wilcox G, Soh S, Chakraborty S, Scardino PT, Wheeler TM. Patterns of high-grade prostatic intraepithelial neoplasia associated with clinically aggressive prostate cancer. Hum Pathol 1998;29:1119–23. [PubMed: 9781651]

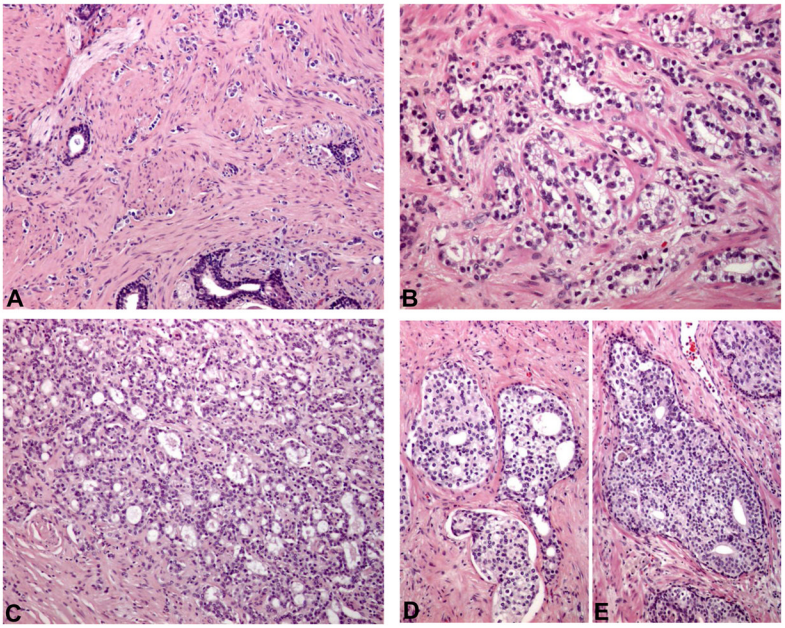

Fig. 1.
Tumor architecture of preoperatively treated prostate cancer: (a) Single cells, cell cords, and cell clusters; (b) small glands; (c) fused glands; (d) cribriform pattern; (e) intraductal spread.

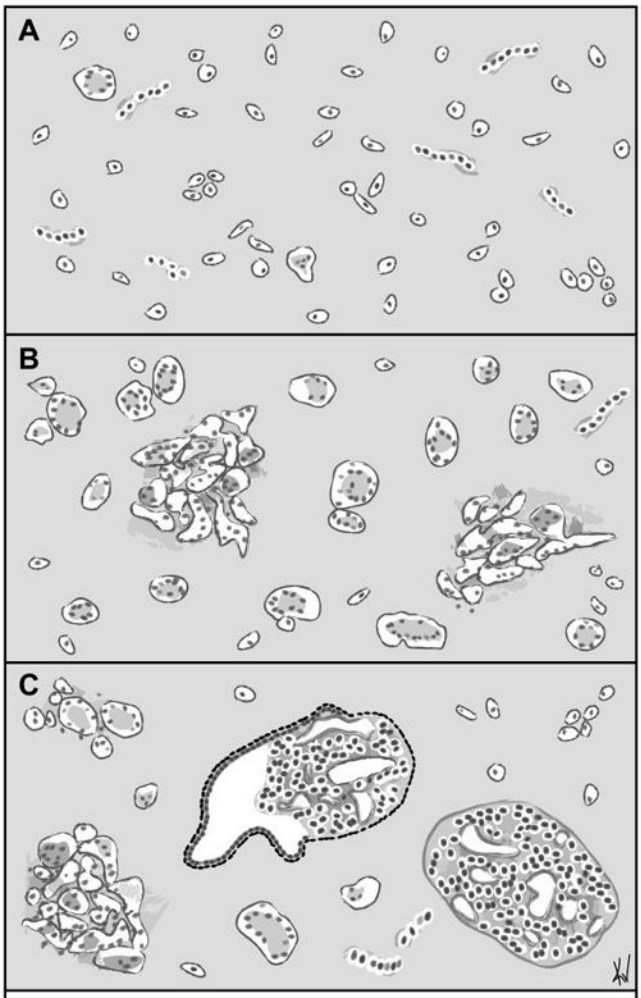

Proposed Grouping of Treated Prostate Cancer

Group	Dominant Architectural Pattern	Cribriform Pattern or Intraductal Spread
A	Cell clusters/cords, isolated cells	Absent
B	Small glands, fused glands	Absent
C	Any	Present

Fig. 2.

Proposed grouping. Top: Group A morphology is characterized by the predominance of isolated cells, cell clusters, and cords with complete absence of cribriform pattern or intraductal tumor spread. Middle: Group B morphology is characterized by the predominance of small and/or fused glands with complete absence of cribriform pattern or intraductal tumor spread. Bottom: Group C morphology is defined by the presence of cribriform pattern and/or intraductal tumor spread regardless of other patterns.

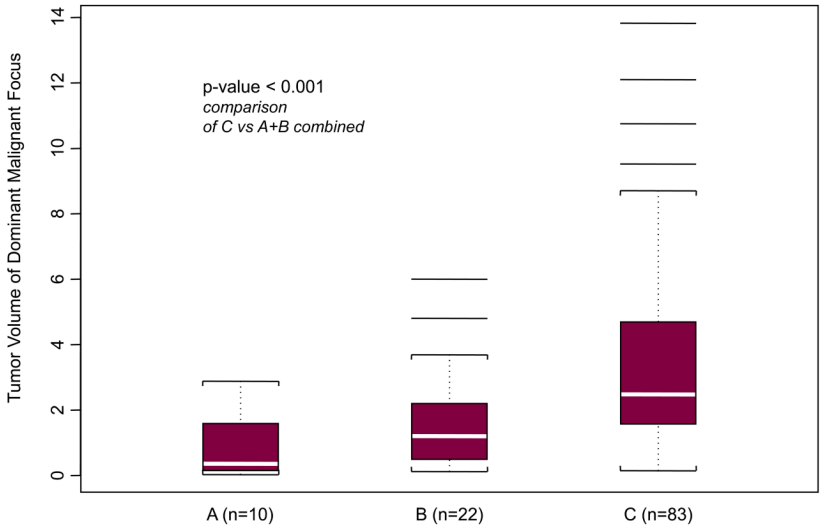

Fig. 3.

Median volumes of the dominant tumor focus according to morphologic group. Group A: 0.36 cm^3 (range: 0.03–2.88 cm^3); group B: 1.20 cm^3 (range: 0.12–6.00 cm^3); group C: 2.48 cm^3 (range: 0.14–13.82); $p < 0.001$ (Kruskal-Wallis test). $P < 0.001$ for groups A and B combined versus group C.

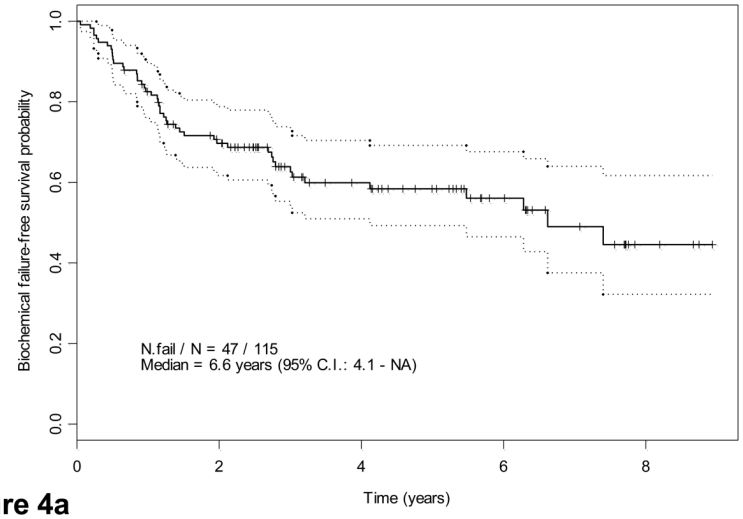

Figure 4a

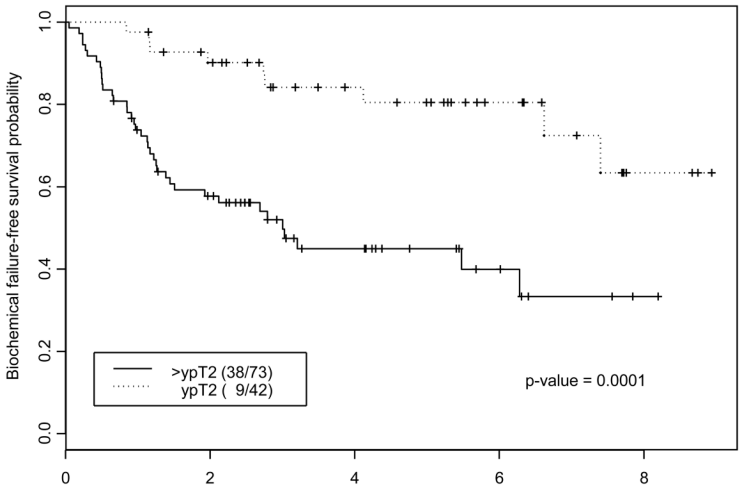

Figure 4b

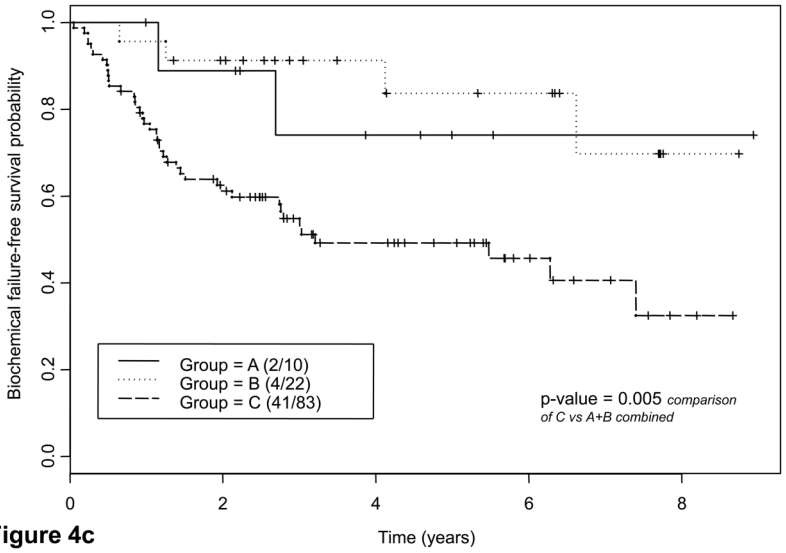

Figure 4c

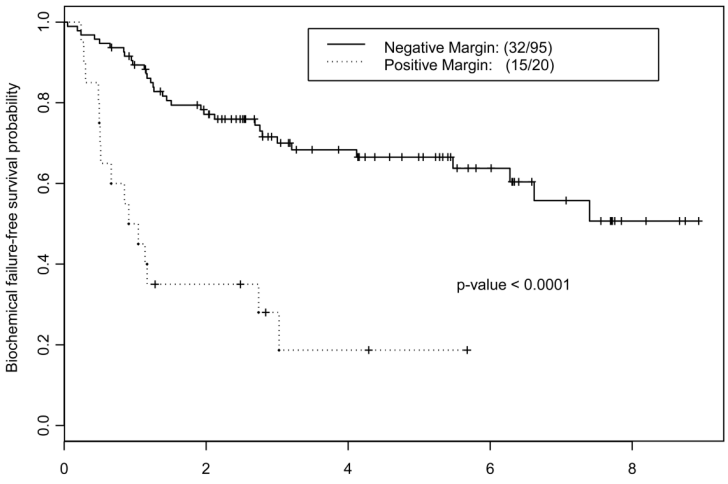

Figure 4d

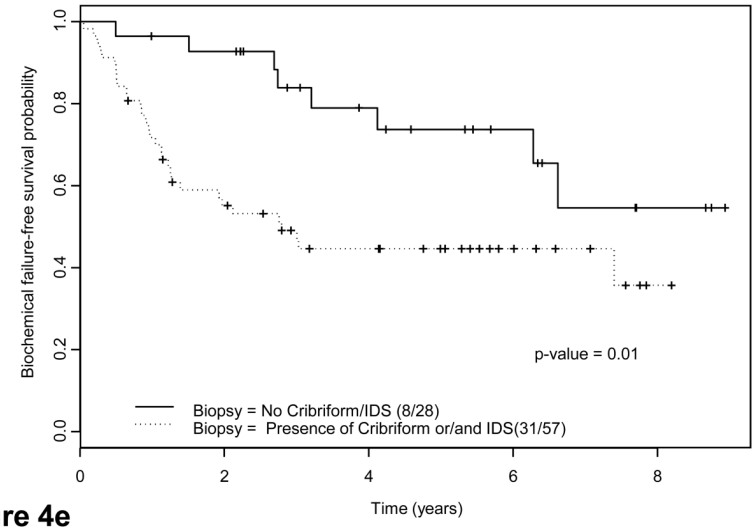

Figure 4e

Fig. 4.

Kaplan-Meier estimates of biochemical failure(BCF)–free survival. Dotted lines above and below represent the confidence intervals (CIs). (a) Kaplan-Meier estimates of BCF-free survival overall, median follow-up 55 mo (range: 42–108 mo) (b) by pathologic stage and (c) by morphologic group A, B, C. $P = 0.001$ for groups A and B combined versus group C (d) by margin status and (e) by biopsy presence versus absence of cribriform pattern and/or intraductal spread (IDS) ($n = 85$; 30 were missing due to lack of complete biopsy data). Note: Kaplan-Meier estimates include as biochemical failure five patients who died of unrelated causes (two in group C and three in groups A and B).

Table 1

Clinical characteristics of 115 preoperatively treated patients with prostate cancer

Age (yr)	**No. (%)**
Median (range)	59 (41–72)
Race	
White	90
Black	19
Hispanic	6
Serum PSA (ng/ml) at diagnosis	
0–4	13 (11)
4.1–10	42 (37)
10.1–20	27 (23)
>20	33 (29)
Clinical stage	
T1c	7 (6)
T2a	25 (22)
T2b	10 (9)
T2c	27 (23)
T3a	17 (15)
T3b	29 (25)
Preoperative treatment	
AA	30
AA + KAVE	57
AA + docetaxel + imatinib	28

AA = androgen ablation; KAVE = ketoconazole, doxorubicin, vinblastine, and estramustine; PSA = prostate-specific antigen.

Table 2

Pathologic characteristics of pretreatment prostate needle biopsies and post-treatment prostatectomy specimens from 115 men with preoperatively treated prostate cancer

Prostate needle biopsies	**No. (%)**
Gleason score	
7 (3 + 4)	14 (12)
7 (4 + 3)	19 (17)
≥ 8	82 (71)
Prostatectomy specimens	
Tumor focality	
Unifocal	74 (64)
Multifocal	41 (36)
Zonal origin of dominant tumor focus	
Peripheral	82 (71)
Transition	14 (12)
Undetermined	19 (17)
Surgical margins	
Positive	20 (17)
Negative	95 (83)
Pathologic stage*	
Organ confined (ypT2N0)	42 (36)
Extraprostatic extension (ypT3aN0)	9 (8)
Seminal vesicle invasion (ypT3bN0)	32 (28)
Pelvic lymph node metastasis (ypT[any]N1)	32 (28)

* "y" signifies preoperatively treated tissue.

Table 3

Architectural and stromal features

Architectural features	0 (%)	1 (%)	2 (%)	3 (%)	Any (%)
Fused glands	5 (4.3)	21 (18.3)	43 (37.4)	46 (40)	110 (95.7)
Cell clusters	5 (4.4)	37 (32.2)	45 (39.1)	28 (24.3)	110 (95.7)
Small glands	13 (11.3)	28 (24.4)	39 (33.9)	35 (30.4)	102 (88.7)
Cell cords	20 (17.3)	32 (27.8)	37 (32.1)	26 (22.6)	95 (82.7)
Isolated cells	31 (27)	35 (30.4)	31 (27)	18 (15.7)	84 (73)
Intraductal spread	45 (39.1)	43 (37.4)	23 (20)	4 (3.5)	70 (60.9)
Cribriform pattern	48 (41.7)	38 (33)	20 (17.4)	9 (7.8)	67 (58.3)
Solid sheets	113 (98)	2 (2)	0	0	2 (2)
Stromal features					
Stromal increase	2 (1.7)	54 (47)	52 (45.2)	7 (6.1)	113 (98.3)
Stromal hypervascularity	8 (6.9)	70 (60.9)	35 (30.4)	2 (1.7)	107 (93.1)
Stromal hypercellularity	33 (28.7)	63 (54.8)	18 (15.6)	1 (0.9)	82 (71.3)
Absent lining	74 (64.3)	28 (24.3)	7 (6.1)	6 (5.2)	41 (35.7)
Stromal mucin	82 (71.3)	24 (20.9)	5 (43.5)	4 (3.5)	33 (28.7)

0 = absent; 1 = present to a minor degree; 2 = present to a considerable degree; 3 = present to an extensive degree.

Table 4

Associations among proposed grouping, pathologic disease stage, pretreatment Gleason score, and pretreatment presence of cribriform pattern and/or intraductal spread

Pathologic stage*	**Group A or B**	**Group C**
Higher than ypT2	10	63
ypT2	22	20
Pretreatment biopsy Gleason score†		
7	10	23
>7	22	60
Cribriform pattern or intraductal spread in pretreatment biopsy‡		
Present	6	51
Absent	16	12

*$p < 0.0001$ by Fisher exact test; “y” signifies preoperatively treated tissue.

†$p = 0.65$ by Fisher exact test.

‡$p < 0.001$ by Fisher exact test in 85 of 115 available biopsy slides.

Table 5

Patients with biochemical relapse stratified by proposed grouping and pathologic stage

Category / Pathologic stage*	A	B	C	Total relapses per pathologic stage [%]
Organ confined (ypT2N0)	1 (8)	0 (14)	5 (20)	6 (42) [14]
EPE/SVI (ypT3N0)	1 (2)	0 (5)	13 (34)	14 (41) [34]
Lymph node positive (ypT[any]N1)	0	2 (3)	20 (29)	22 (32) [69]
Total relapses per category [%]	2 (10) [20]	2 (22) [9]	38 (83) [46]	42 (115) [37]

EPE = extraprostatic extension; SVI = seminal vesicle invasion; ( ) = total no. cases within that category; [ ] = percentage.

*"y" signifies preoperatively treated tissue.

Table 6

Multivariate analysis of potential predictors of relapse

Variable	Coefficient	SE	Relative risk	*p* value
Age	−0.03	0.02	0.97	0.17
Pathologic stage ypT2 (vs others)	−0.62	0.45	0.54	0.16
Margin positive (vs negative)	0.93	0.37	2.53	0.01
Treatment 3, 4 (vs 1, 2)*	−0.61	0.32	0.54	0.06
Gleason score >7 (vs ≤7)	0.48	0.38	1.62	0.21
PSA >10 (vs ≤10)	0.26	0.36	1.30	0.47
Clinical stage T3a, T3b (vs others)	0.08	0.35	1.08	0.83
Group C (vs A or B)	1.03	0.52	2.79	0.05
Total tumor volume	0.05	0.06	1.05	0.40
Reduced model with only significant variables included				
Margin positive (vs negative)	1.27	0.34	3.56	<0.001
Group C (vs A or B)	1.09	0.46	2.98	0.02
Treatment 3, 4 (vs 1, 2)*	−0.65	0.32	0.52	0.04

PSA = prostate-specific antigen; SE = standard error.

*Treatment 1, 2 = androgen ablation plus KAVE (ketoconazole, doxorubicin, vinblastine, and estramustine) (two different trials); treatment 3 = androgen ablation alone; treatment 4 = androgen ablation plus docetaxel plus imatinib.